

Raspberry PhenoSet: A Phenology-based Dataset for Automated Growth Detection and Yield Estimation

Parham Jafary, Anna Bazangeya, Michelle Pham,
Lesley G. Campbell, Sajad Saeedi, Kourosh Zareinia, Habiba Bougherara

Abstract—The future of the agriculture industry is intertwined with automation. Accurate fruit detection, yield estimation, and harvest time estimation are crucial for optimizing agricultural practices. These tasks can be carried out by robots to reduce labour costs and improve the efficiency of the process. To do so, deep learning models should be trained to perform knowledge-based tasks. Which outlines the importance of contributing valuable data to the literature. In this paper, we introduce Raspberry PhenoSet, a phenology-based dataset designed for detecting and segmenting raspberry fruit across seven developmental stages. To the best of our knowledge, Raspberry PhenoSet is the first fruit dataset to integrate biology-based classification with fruit detection tasks, offering valuable insights for yield estimation and precise harvest timing. This dataset contains 1,853 high-resolution images, the highest quality in the literature, captured under controlled artificial lighting in a vertical farm. The dataset has a total of 6,907 instances of mask annotations, manually labelled to reflect the seven phenology stages. We have also benchmarked Raspberry PhenoSet using several state-of-the-art deep learning models, including YOLOv8, YOLOv10, RT-DETR, and Mask R-CNN, to provide a comprehensive evaluation of their performance on the dataset. Our results highlight the challenges of distinguishing subtle phenology stages and underscore the potential of Raspberry PhenoSet for both deep learning model development and practical robotic applications in agriculture, particularly in yield prediction and supply chain management. The dataset and the trained models are publicly available for future studies.

Index Terms—Raspberry dataset, Phenology stages, Fruit detection, Yield estimation, Agricultural Automation, Farm robot, Computer Vision for Automation.

I. INTRODUCTION

ESTIMATING when and how much yield a farm will produce is critical in the food supply chain. Farmers face financial penalties due to contractual obligations for under and over-delivering perishable goods to retailers and distributors. Another benefit of accurate yield estimation is that it supports a better market position and pricing stability. Shortages may cause price hikes and dissatisfaction among buyers, while surpluses can force distributors to sell at lower prices, negatively impacting the market position of both farmers and distributors. Finally, accurate estimates allow for better transportation, storage, and sales planning, reducing the costs associated with underutilized logistics or the need for last-minute adjustments [1].

To achieve accurate yield estimation, farmers need to have a deep understanding of the speed of fruit or vegetable ripening and developmental stages of the fruit (phenology) as well as the labour to conduct regular visual inspections to monitor crop development, which is a time-consuming and

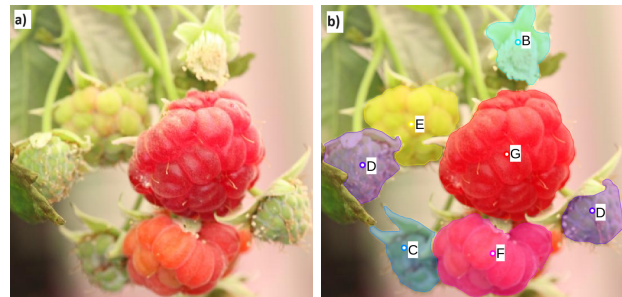


Fig. 1. A sample image from the Raspberry PhenoSet, taken at the vertical farming facility at the Center of Urban Innovation of Toronto Metropolitan University. a) Original image with no annotations. b) Mask annotations of all instances present in the image; Labels A-G correspond to the seven phenology stages of raspberries.

costly task. However, finding specific targets using visual observations is a well-studied task in computer vision, called object detection [2]. In some cases such as fruit sorting, a fixed camera and a computer are sufficient to carry out [3], [4]. However, in many cases of fruit detection and yield estimation (such as raspberries) the leaves and branches grow randomly, therefore, a fixed camera would be incapable of detecting the desired targets. This outlines the need to have a robot with a camera attached to its arm to move around and capture images from appropriate angles. For robots to predict yield, they need to detect fruits and classify each fruit into a developmental stage. With recent advances in parallel computing, artificial intelligence models (especially deep learning (DL) models) have outperformed other techniques and have become the state-of-the-art method in the field [2]. Yet, deep neural networks (DNNs) feed on large datasets and they need to be trained on a task-specific level to achieve desired outcomes (see Fig. 1). We can leverage transfer learning [5] and fine-tune a network that is pre-trained on a large dataset using a relatively small dataset. Therefore, developing task-specific datasets is crucial to make automation feasible using DNNs.

Large and publicly available datasets such as COCO [6] and LVIS [7] are not fruit-specific, and lack the proper environment, illumination, and abundance. Many fruit-specific datasets such as [8]–[12] are not publicly available. There are available datasets on strawberries, grapes, and tomatoes [8], [10], [12]–[15], however, they possess only a few hundred images or their images have low resolution both of which prevent achieving good accuracy with DL models. More importantly, even the datasets that are fruit-specific, publicly available, and contain a sufficient number of images, lack

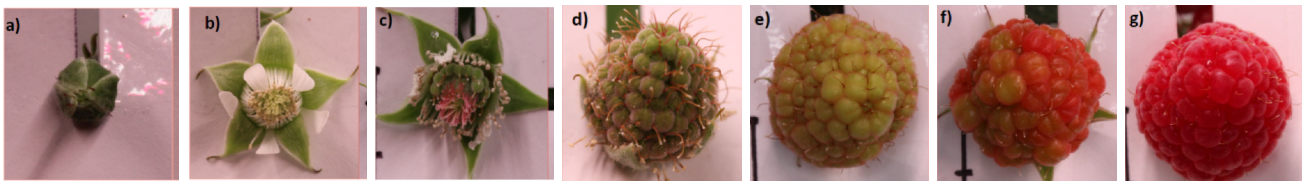


Fig. 2. Phenology reference of raspberry development stages used for annotating the images. The stages are labelled a-g, representing the seven development stages. a) Buds b) Open Flower c) Fruit Initiation d) Green Fruit e) Growing Fruit (yellow colour) f) Semi-mature (pink) fruit g) Mature (red) fruit

biological relevance from which the timing of harvest cannot be elucidated. For instance, Afonso et al. [16] have labelled their tomato dataset simply by colour i.e. green, red, etc. and Cossio-Montefinale et al. [17] have too broad categories (green, unripe, ripe) to derive meaningful data to determine precise harvest dates. This makes them unpractical from a supply chain and yield estimation point of view. Moreover, object detection models are sensitive to illumination and all of the the previous datasets were captured in conventional farms or greenhouses which use sunlight, whereas vertical farms use artificial lights and have a different illumination.

In this paper, we present the Raspberry PhenoSet for raspberry detection, segmentation, and yield estimation. Raspberry PhenoSet is a large and high-quality dataset with 1853 images and 6907 mask annotations, that were manually labelled. The images are provided in two different sizes, a smaller size suitable for current widely-used GPUs and a larger size suitable for future hardware upgrades. To the best of our knowledge, Raspberry PhenoSet is the first phenology-based dataset, the first dataset gathered in a vertical farming environment, and also has the largest image size amongst the fruit datasets [17] and it is publicly available¹. The images are annotated and classified according to the development stages of raspberry plants (see Fig. 2), i.e. the remaining days before harvest are known for each class, making them suitable to estimate the yield and the harvest time precisely, therefore, fulfilling the supply chain needs discussed earlier.

In the rest of the paper, we discuss the recent advances in the field in Sec. II, provide the details and considerations of creating the dataset in Sec. III, describe the models and metrics used for the evaluation of the dataset in Sec. IV, present the results and benchmark the dataset in Sec. V, discuss the results and performance of different models in Sec. VI, and finally provide conclusions and recommendations in Sec. VII.

II. RELATED WORKS

DNNs perform well when distinguishing among very different classes. For example, Sa et al. [28] used Faster R-CNN to distinguish among fruits, achieving an F1-score of 0.83 across all classes. The precision and reliability of DNNs in fruit detection have made them useful for automating various tasks. For instance, Zhu et al. [29] used DNNs to detect lesions on apples. Other researchers have employed DNNs to characterize fruit ripeness [16], [30]. Fan et al. [9] used YOLOv5 to classify strawberries as either immature, close to maturity, mature, or unmarketable. Moreover, fruit detection is

crucial for autonomous harvesting [23], [31]. Arad et al. [32] developed an autonomous robot that used RGB-D images to harvest sweet peppers.

Datasets are essential for training DNN models. Effective training requires a dataset with a sufficiently large and diverse set of samples to represent various scenarios and challenges. The number of images needed for practical applications depends on factors such as the type of fruit, the similarity of the classes with each other and the similarity of the classes with the background; generally, more images result in better generalization capabilities. Fruits like apples [18], [33], oranges [34], and cherries [35] grow on trees with highly irregular distributions due to occlusion and irregular growth patterns. In contrast, plants grown in structured environments, like tomatoes in greenhouses or grape clusters on trellises, show less occlusion and more regular distributions [10], [13]. Another important feature of a dataset is the size of the images and the size of each fruit in the images, as it influences the level of detail for each instance. High-resolution images offer either greater detail for each fruit or cover a broader field of view [17]. Nonetheless, training DL models with high-resolution images requires stronger GPUs as the required memory increases.

Labelling each visible fruit in each image makes building a dataset expensive and time-consuming, therefore, public datasets are important contributions both for academic research and industrial practice. For example, the ACFR dataset published by Suchet et al. [36], includes 1,120, 1,964, and 620 annotated images of apples, mangoes, and almonds, respectively. The apple and mango images were taken using a mobile robot, while the almond images were captured using a handheld camera. Despite the relatively high number of images, this dataset has low resolution, with a maximum of 500×500 pixels for mango images and 308×202 pixels for apple and almond images. These images were taken closely to compensate for the resolution, but this may result in poor performance if the network is given an image from a further distance. Häni et al. [22] published the MinneApple dataset, containing 1,000 labelled images of apple trees. These images were acquired using a handheld smartphone camera in different apple plantations, including green and red apple varieties. Unlike most fruit datasets, the annotations for each apple are in mask format, allowing for fruit detection and segmentation. Another public dataset created by Bhusal et al. [21], consists of 2,298 images of apples with bounding box (BB) annotations, taken in an apple orchard using a camera mounted on a mobile robot. Additionally, Santos et al. [14] published a dataset for grape detection and segmentation, labelling 300 images using

¹<https://sites.google.com/view/raspberry-phenoset>

TABLE I
AN OVERVIEW OF THE FRUIT DETECTION DATASETS IN THE LITERATURE

Fruit	Dataset Size	Image Size	Farm Type	Availability	Phenology-based
Apples	300	640 × 640	Conventional	Private	No [8]
Apples	1,386	600 × 400	Conventional	Private	No [18]
Apples	267	416 × 416	Conventional	Private	No [19]
Apples	1,200	416 × 416	Conventional	Private	No [20]
Apples	2,298	1280 × 960	Conventional	Public	No [21]
Apples	1,000	1280 × 720	Conventional	Public	No [22]
Apples	285	640 × 480	Greenhouse	Private	No [23]
Citrus	4,855	1920 × 1080	Conventional	Public	No [24]
Citrus	579	2448 × 3264	Conventional	Public	No [25]
Grapes	300	1365 × 2048	Conventional	Public	No [14]
Grapes	961	300 × 450	Conventional	Private	No [12]
Mangoes	1,100	800 × 600	Conventional	Private	No [11]
Raspberry	2039	1773 × 1773	Conventional	Public	No [26]
Strawberries	2,400	Not Available	Conventional	Private	No [9]
Strawberries	177	1280 × 720	Greenhouse	Public	No [13]
Tomatoes	996	512 × 512	Greenhouse	Private	No [10]
Tomatoes	318	504 × 377	Greenhouse	Private	No [27]
Tomatoes	250	2000 × 2000	Greenhouse	Public	No [15]
Raspberry(Current Study)	1853	5184 × 3456	Vertical Farm	Public	Yes

a novel method for labelling clusters of grapes.

As mentioned in Sec. I and provided in Table I, previous datasets are either not publicly available, contain a low number of images, or lack biologically informed labels, making them of limited use to supply chain applications. The Raspberry PhenoSet addresses these issues by providing a large, high-resolution dataset specifically designed for detection and segmentation tasks. It is the first dataset to include annotations based on plant phenology, enabling accurate yield estimation and forecasting for farmers. This dataset bridges the gap between academic research and practice, encouraging the agriculture industry to adopt robotics and computer vision to enhance performance and profitability.

III. RASPBERRY PHENOSET

Since the images are annotated based on phenological stages, some classes have subtle differences, making the dataset challenging even for state-of-the-art object detection models. Top object detection and segmentation models were trained using different backbones to provide a comprehensive benchmark for the Raspberry PhenoSet. Annotations are provided both in bounding box and mask format, making the dataset suitable for both object detection and segmentation algorithms. Thus, Raspberry PhenoSet is a practical and valuable tool for both farmers and deep-learning model developers.

In this section, we explore various aspects of the Raspberry PhenoSet focusing on the image capture methodology, classification criteria, and statistical properties of the dataset.

A. Data Acquisition

A detailed study of the phenological stages of raspberries was carried out by taking photographs of the plants throughout the growth period and the results are presented in Table II. Three raspberry cultivars, Polana, Prelude, and Joan J were grown for this study in our vertical farm facility at the Center for Urban Innovation at Toronto Metropolitan University. The images were taken with a Canon EOS Rebel T3i at a

5184×3456 resolution which has a variable focal length of 18-55 *mm* and an electronically-controlled, focal-plane shutter; The camera was set on Scene Intelligent Automatic Mode which determined the appropriate aperture, shutter speed, and ISO to adjust exposure. Metadata of each image is saved and accessible in its properties; camera calibration results are also provided on the website. accessible Overhead plant lighting were the main source of lighting during the photo sessions. Three photo sessions were carried out per week for three months, from January 2024 to March 2024 and a total of 72 person-hour time was spent on it.

The vertical farming facility uses artificial lights instead of sunlight, providing constant light intensity during the daytime. Nonetheless, due to plants growing and fruiting in various directions, the pictures were taken from various angles, and therefore the dataset includes photos of fruits with different levels of illumination. Also, due to the presence of air nozzles, irrigation systems, and other subsystems of the vertical farm, many images are occluded with unwanted obstacles. The photos were taken at various distances, ranging from 20 to 100*cm*, from the target objects, resulting in various sizes for the objects of interest. Moreover, since the camera was set on auto-focus condition, some objects of interest became blurry. All of these factors contributed to having a realistic and diverse dataset that represents the challenges of image analysis in vertical farming environments.

TABLE II
PHENOLOGY-BASED CORRELATION OF GROWTH STAGE AND HARVEST TIME FOR DIFFERENT RASPBERRY CULTIVARS

Phenology Stage	Days Left to Harvest for Cultivars		
	Polana	Prelude	Joan J
A	31.9	33.3	28.1
B	28.5	31.1	25.6
C	25.1	27.5	23.6
D	13.6	16.5	13.5
E	5.0	3.2	3.3
F	2.8	0.5	n/a
G	0.0	0.0	0.0

TABLE III
SPECIFICATIONS OF RASPBERRY PHENOSET ANNOTATIONS

Phenology stage	Total images	Total annotations	Mean BB width [px]	Mean BB height [px]	Average annotated area [px ²]	Image area percentage
A	187	1322	315.03	352.87	135075.68	0.75
B	452	1428	688.25	668.81	570569.68	3.18
C	373	1424	549.07	562.2	404791.96	2.26
D	260	1267	716.96	689.11	602083.71	3.36
E	218	509	661.56	646.58	544447.26	3.04
F	148	386	726.56	700.8	652934.44	3.64
G	215	571	508.94	496.18	325503.06	1.82
Total	1853	6907	595.2	588.1	462200.83	2.58

B. Classification Criteria

The growth stages of the raspberry plant were identified, resulting in seven classes as shown in Fig. 2. These classes represent different levels of maturity of raspberries and correspond to the described BBCH-scale phenological stages in the timeline of raspberry growth [37]. These classes are:

- Stage A: Floral bud;
- Stage B: Open flower with white petals;
- Stage C: Green fruit initiation with very small drupelets;
- Stage D: Green fruit with drupelet growth;
- Stage E: Growing fruit with colour changing to yellow;
- Stage F: Semi-mature pink fruit;
- Stage G: Mature red fruit.

A total of 2200 images were captured, after discarding the images with a high degree of blurriness or other corruption, 1853 images were selected for annotation. The images were labelled A-G, based on the overall phenology timeline, to provide a statistical report (please see Table III). However, this does not imply that those images contain instances of a specific phenology stage. Due to the continuous development of new buds, flowers and fruits throughout the documentation process, more than one phenology stage is present in most of the images.

All visible and recognizable instances of buds, flowers, and fruits in all photographs were annotated and categorized into one of the aforementioned stages. All images were manually annotated using the V7Labs platform². Buds, flowers, and fruits were labelled according to the phenology reference given in Fig. 2. The classes were labelled using the polygon format to ensure that the details were captured. The annotation process took 160 person-hour time and was carried out by the first author.

TABLE IV
HYPER-PARAMETERS OF IMPLEMENTED MODELS

Model	Backbone/Scale	Batch Size	Learning Rate	Weight Decay	Epochs
Faster R-CNN	ResNet-50	8	0.001	0.0001	150
Faster R-CNN	ResNet-101	6	0.001	0.0001	150
Mask R-CNN	ResNet-50	8	0.001	0.0001	150
Mask R-CNN	ResNet-101	4	0.001	0.0001	150
YOLOv8	yolov8-m/l	16	0.01-0.0001	0.0005	100
YOLOv8	yolov8-x	12	0.01-0.0001	0.0005	100
YOLOv10	yolov10-l	12	0.01-0.0001	0.0005	100
YOLOv10	yolov10-x	9	0.01-0.0001	0.0005	100
RT-DETR	rt detr-l/x	12	0.001	0.0005	100

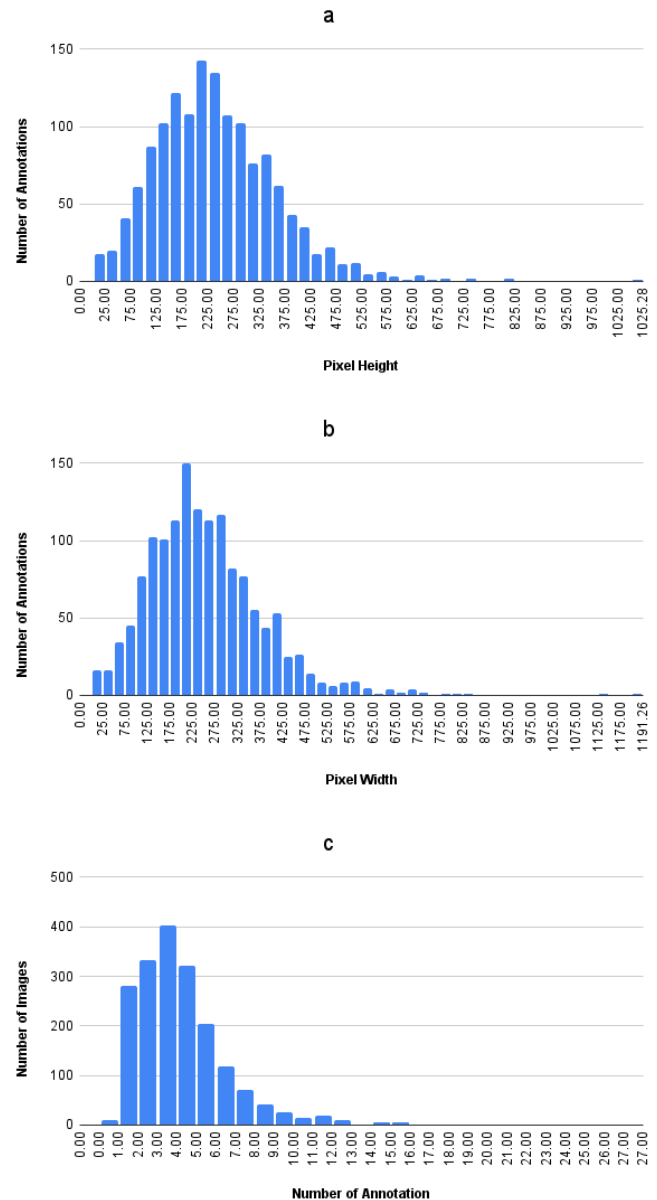


Fig. 3. Histogram of Annotations in Raspberry PhenoSet a) Number of Annotations vs. Pixel Heights b) Number of Annotations vs. Pixel Widths c) Number of Images vs. Number of Annotations per Image

²<https://darwin.v7labs.com>

TABLE V
PERFORMANCE OF DIFFERENT NETWORKS ON THE RASPBERRY PHENOSET

Network	Backbone/Scale	Precision	Recall	AP50	mAP50-95	F1
YOLOv8	yolov8-m	0.683	0.661	0.698	0.542	0.672
YOLOv8	yolov8-l	0.694	0.674	0.700	0.544	0.684
YOLOv8	yolov8-x	0.721	0.668	0.717	0.550	0.693
YOLOv10	yolov10-l	0.661	0.599	0.652	0.460	0.628
YOLOv10	yolov10-x	0.602	0.653	0.647	0.457	0.626
RT-DETR	rt detr-l	0.681	0.700	0.659	0.512	0.690
RT-DETR	rt detr-x	0.682	0.704	0.674	0.506	0.693
Faster R-CNN	ResNet-50	0.634	0.583	0.620	0.446	0.607
Faster R-CNN	ResNet-101	0.594	0.577	0.591	0.430	0.585
Mask R-CNN	ResNet-50	0.628	0.580	0.617	0.454	0.603
Mask R-CNN	ResNet-101	0.583	0.575	0.571	0.442	0.579

C. Statistical report

Table III shows the number of images and annotations per class of the Raspberry PhenoSet. The dataset consists of 1853 images and has 6907 annotations. The first three stages have a higher number of annotations due to the continuous emergence of new buds throughout the three-month growth period. The images in each class were randomly split into 70%, 15%, and 15% portions for training, validation, and testing purposes, respectively.

Due to capturing images at various distances from the plants, the Raspberry PhenoSet includes annotations at various sizes starting from 20 pixels and reaching more than 1500 pixels. This allows the networks to learn the target objects' details and shape factors properly.

IV. EVALUATION OF THE DATASET

Different state-of-the-art DL object detection and segmentation networks were chosen based on their characteristics and their performance was evaluated on the Raspberry PhenoSet. The implemented deep learning models are described in Sec. IV-A, and the evaluation metrics are presented in Sec. IV-B.

A. Deep Learning Models

State-of-the-art object detection models can be categorized as either one-stage or two-stage models. One-stage detectors perform object detection in a single pass through the network, predicting bounding boxes and class probabilities directly from the input image. One-stage detectors are typically faster and more suitable for real-time applications because they process images in a single forward pass [38]. Two-stage detectors use a more complex approach, first generating region proposals and then refining these proposals to detect objects. Two-stage detectors generally achieve higher accuracy and better performance in terms of localization and classification, particularly for small and densely packed objects [39]. The networks with the highest performance of both categories were used to benchmark the dataset and to provide a comprehensive comparison.

1) *One-stage networks*: This field is dominated by different versions of the YOLO network [2]. In this paper, YOLOv10, YOLOv8, and RT-DETR were chosen as the one-stage object detection models. YOLOv10 was chosen due to its real-time

capabilities [40], YOLOv8 was chosen due to having a greater number of parameters [41], and RT-DETR was chosen since it uses a transformer-based architecture which is different from YOLOs that are based on convolutional neural networks [42].

2) *Two-stage networks*: Faster R-CNN and Mask R-CNN are the top two-stage networks in the literature and they are commonly used with ResNet-50 and ResNet-101 backbones [39]. Faster R-CNN was primarily designed for object detection, while Mask R-CNN extends Faster R-CNN to add instance segmentation, enabling it not only to detect objects but also to generate a precise segmentation mask for each detected object [43], [44]. Although ResNet-101 is a larger network and is expected to perform better, both backbones have been tested to provide a comparison.

B. Evaluation Metrics

To evaluate and compare the performance of different models the dataset was randomly split into three subsets of training, validation, and testing with them having a share of 70, 15, 15 percent of all the images. The following metrics were used to quantify the models' performance.

1) Precision (P): A performance metric calculated by dividing the number of true positive predictions by the sum of the true positives and false positives.

2) Recall (R): Another performance metric indicating how often the model detects positive instances correctly and is calculated by dividing the number of true positives by the sum of true positives and false negatives.

3) Average Precision (AP): A more comprehensive performance metric used primarily to evaluate models in object detection and other classification tasks. AP summarizes the precision-recall curve by calculating the area under the curve. AP provides a single value representing the model's ability to balance precision and recall across different thresholds.

4) Mean Average Precision (mAP): The mean of the AP values for multiple classes, and is useful in multi-class object detection to provide a comprehensive evaluation of the model's performance across all classes.

5) F1-Score is the harmonic mean of precision and recall. It provides a single metric that balances both precision and recall and is especially useful when the class distribution is imbalanced.

All models were trained locally on an Nvidia Geforce RTX-3060 GPU, and the networks' hyper-parameters were adjusted

TABLE VI
PERFORMANCE OF YOLOV8-X ON THE RASPBERRY PHENOSSET

Class	Precision	Recall	AP50	mAP50-95	F1
A	0.802	0.819	0.855	0.679	0.810
B	0.773	0.635	0.729	0.493	0.697
C	0.621	0.534	0.592	0.367	0.574
D	0.641	0.652	0.677	0.482	0.646
E	0.731	0.569	0.64	0.506	0.640
F	0.849	0.577	0.678	0.599	0.687
G	0.632	0.891	0.85	0.712	0.739
Overall	0.721	0.668	0.717	0.548	0.693

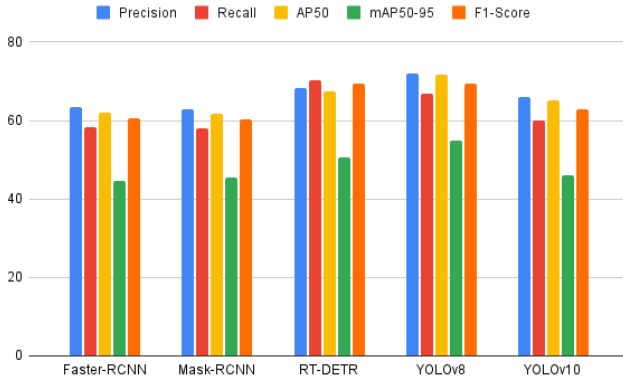


Fig. 4. Best Performance of Different Networks on the Raspberry PhenoSet, Visualizing the Suitability of YOLOv8 and RT-DETR for Fruit Detection Applications

to make the training feasible, due to memory limits, and to improve the performance of the networks. For each model, the number of epochs with the best performance is reported. A summary of the hyper-parameters is given in Table IV.

V. RASPBERRY PHENOSSET BENCHMARKS

The results from benchmarking the Raspberry PhenoSet with the state-of-the-art one-stage and two-stage object detection models are presented in this section. As discussed earlier, the images were classified into seven categories based on their phenology stage. This allows us to test the ability of different deep-learning models to detect precise phenological stages. Some of these categories have subtle differences and some have major differences in shape, size, and colour. In Sec. V-A the performance results of different networks are presented.

A. Performance of Different Models

To provide a comprehensive benchmark, different backbones and scales of each model were implemented. To analyze one-stage models, medium, large and extra large scales of YOLOv8 and large and extra large scales of YOLOv10 were trained. RT-DETR comes with two scales, large and extra large, and both of them were trained on the dataset. To study the performance of two-stage models, Faster R-CNN and Mask R-CNN were trained using the two widely used backbones ResNet-50 and ResNet-101. The performance of the networks on the Raspberry PhenoSet can be seen in Table V.

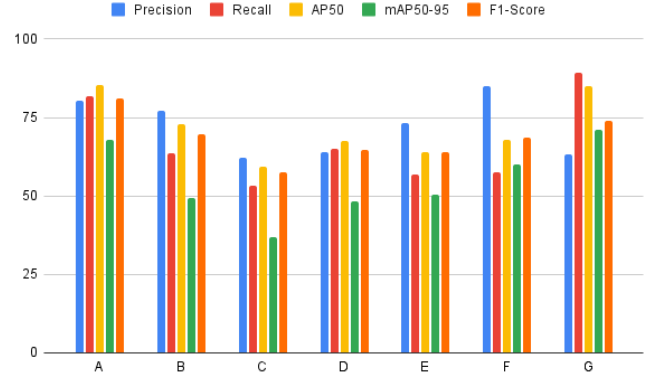


Fig. 5. Performance of YOLOv8-x on Each Class of the Raspberry PhenoSet, Showing the Model's Ability to Distinguish Each Phenology Stage

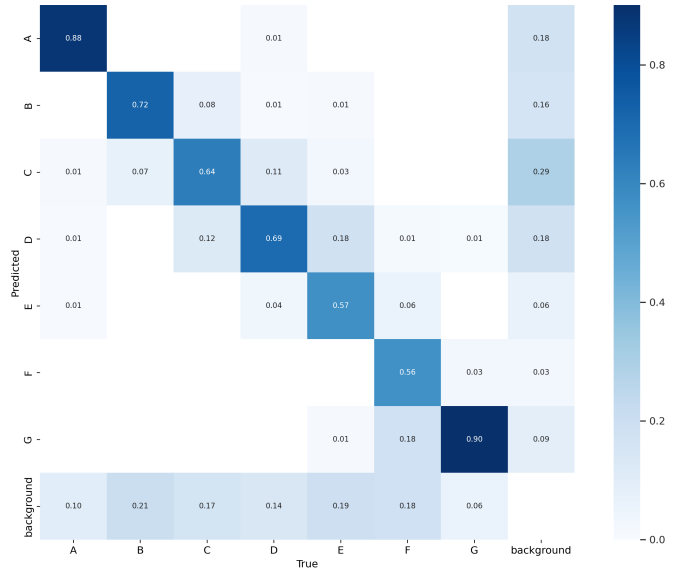


Fig. 6. Normalized Confusion Matrix of YOLOv8-x, Showing the Distribution of False Detection Across Different Classes

It can be seen that YOLOv8-x has the highest precision, average precision, and mean average precision while RT-DETR-x has the highest F1 score. Table V also shows that having a larger network does not necessarily yield better performance within the available computational resource. In training the models with ResNet-101, the computational overhead forced us to use different hyper-parameters which led to a lower performance than the models with ResNet-50.

VI. DISCUSSION

Based on Table V, it can be seen that the two-stage models, Faster R-CNN and Mask R-CNN have lower performance than YOLOs and RT-DETR. Moreover, by changing their backbone and increasing their parameters, their performance depreciates. This is due to their computational overhead which prevents training with a high batch size (see Table IV). Fig. 4 provides a visual representation of different networks' performance, in which the best configuration with the best performance of each network is used. With this visual comparison, one can

conclude that YOLOs and RT-DETR are more suitable for fruit detection and classification purposes.

As mentioned earlier, RT-DETR has a transformer-based architecture which requires more computational resources. An advantage of this model is that the computational overhead increases marginally from its large to extra-large scale and training was feasible with a batch size of 12 for both scales. Table V shows that RT-DETR has a better performance than YOLOv10 and has the best overall recall and F1 score among all networks; nonetheless, it falls behind YOLOv8 in terms of precision.

Results indicate that as the scale of YOLOv8 increases, its performance improves. The advantage of this model is that increasing its scale does not increase the computational overhead significantly and a batch size of 16 can be trained on medium and large scales; even with the extra-large scale, a batch size of 12 was feasible. On the other hand, YOLOv10, which has better real-time performance, requires more GPU memory in larger scales, thus the batch size was lowered for compensation, resulting in it falling behind YOLOv8 in terms of all performance metrics.

Overall the best performance was achieved with YOLOv8-x and its detailed results are presented in Table VI and Fig. 5. The results show that the highest precision was achieved with the phenology stages A and F while stages C, D, and G had a lower precision. The confusion matrix illustrated in Fig. 6 provides insights about the model's performance. For instance, phenology stage G has a low precision but it also has a high accuracy value in the confusion matrix. This is due to having a high recall value, meaning that class G is being predicted frequently, with some predictions being incorrect and leading to low precision, while most actual stage G instances are correctly detected, leading to a high accuracy value.

The confusion matrix (Fig. 6) shows that phenology stages with subtle differences such as D and E were confused with each other. Moreover, it can be seen that there are false negatives (an object of interest not being detected) in all stages. Further investigation showed that these false negatives are mostly caused by mistaking small annotations (small green buds and white flowers) with background (including leaves and white shelving) by the model. This sheds some light on potential bottleneck improvements (like changing the color of the shelving or searching for alternative spectra that differentiate flowers, buds and leaves [45], [46]).

Raspberry PhenoSet can be used for various purposes and applications with countless possibilities in sustainable and autonomous agriculture. An important application would be yield estimation, starting from the budding stage with the ability to refine the forecasted yield as the plants grow to keep fruit buyers apprised of availability. Another application of the dataset would be a goods monitoring system which utilizes a video feed and alerts the user as the harvest time approaches. Finally, the dataset can be used to operate fruit harvester robots, they would find and pick fruit at the right stage of ripeness. Combining models trained with the Raspberry PhenoSet with the Neural Radiance Fields [47], multiple robots can scan the entire farm and provide a 3D map with accurate locations of buds, flowers, and fruits.

Another important purpose would be health monitoring. The dataset was gathered in a vertical farming facility without any pesticides present, therefore, by adding a number unhealthy samples to each class it can easily be adapted to identify pests or fungi for early control.

VII. CONCLUSION

In this study, for the first time, a phenology-based dataset of raspberries was presented. Raspberry PhenoSet has several advantages that make it suitable for both academic research and industrial applications. The dataset has the highest resolution among previous fruit detection datasets, and it is also the first fruit dataset gathered in a vertical farming facility.

Raspberry PhenoSet was gathered as the plants grew and underwent different phenology stages, namely, budding, flowering, and fruiting. Hence, it reflects various challenges present in a vertical farming facility, such as reflections from artificial lights, and occlusions caused by the random growth of stems and leaves. In Raspberry PhenoSet, the images were annotated based on the phenology stages, meaning that each class has a known number of days remaining before reaching its harvest time. This makes the dataset suitable for yield estimation and supply chain management.

The Raspberry PhenoSet offers a variety of applications in sustainable and autonomous agriculture, including yield prediction, real-time growth or health monitoring, and robotic fruit harvesting. It allows for the estimation of fruit yields starting from the budding stage, refining forecasts as the plants grow to keep buyers informed and to preplan transportation and other supply chain needs. Furthermore, the dataset facilitates the operation of robots that can locate and pick fruit at the right ripeness, and it can be used to create a detailed 3D map of the farm. Overall, the Raspberry PhenoSet showcases significant potential to enhance agricultural practices.

State-of-the-art deep learning object detection and classification models were trained using the Raspberry PhenoSet and the results are provided as a baseline for future studies. Although the models have acceptable performance in detecting and classifying phenology stages, results indicate that even the top models struggle to distinguish some of the phenology stages. We believe this makes the Raspberry PhenoSet suitable for researchers developing deep-learning object detection and classification models.

ACKNOWLEDGMENT

This work was supported by funding from the Weston Family Foundation Homegrown Innovation Challenge (SA-10691) and funding from the Natural Sciences and Engineering Research Council of Canada (NSERC).

REFERENCES

- [1] J. B. Adam Diamond, "Moving food along the value chain: Innovations in regional food distribution." *U.S. Dept. of Agriculture, Agricultural Marketing Service. Washington, DC.*, 2012.
- [2] Z. Zou, K. Chen, Z. Shi, Y. Guo, and J. Ye, "Object detection in 20 years: A survey," *Proceedings of the IEEE*, vol. 111, no. 3, pp. 257–276, 2023.

- [3] C. S. Nandi, B. Tudu, and C. Koley, "An automated machine vision based system for fruit sorting and grading," in *2012 Sixth International Conference on Sensing Technology (ICST)*. IEEE, 2012, pp. 195–200.
- [4] M. Duraisamy, R. Govindaraj, N. Mohan, A. Kamalakannan, S. Bindal, and A. Titus, "Performance evaluation of deep learning based mandarin fruit sorting system with industrial camera," in *2022 3rd International Conference on Smart Electronics and Communication (ICOSEC)*, 2022, pp. 1238–1243.
- [5] F. Zhuang, Z. Qi, K. Duan, D. Xi, Y. Zhu, H. Zhu, H. Xiong, and Q. He, "A comprehensive survey on transfer learning," *Proceedings of the IEEE*, vol. 109, no. 1, pp. 43–76, 2020.
- [6] T.-Y. Lin, M. Maire, S. Belongie, J. Hays, P. Perona, D. Ramanan, P. Dollár, and C. L. Zitnick, "Microsoft coco: Common objects in context," in *Computer Vision—ECCV 2014: 13th European Conference, Zurich, Switzerland, September 6–12, 2014, Proceedings, Part V 13*. Springer, 2014, pp. 740–755.
- [7] A. Gupta, P. Dollar, and R. Girshick, "Lvis: A dataset for large vocabulary instance segmentation," in *Proceedings of the IEEE/CVF conference on computer vision and pattern recognition*, 2019, pp. 5356–5364.
- [8] H. Wang, J. Feng, and H. Yin, "Improved method for apple fruit target detection based on yolov5s," *Agriculture*, vol. 13, no. 11, p. 2167, 2023.
- [9] Y. Fan, S. Zhang, K. Feng, K. Qian, Y. Wang, and S. Qin, "Strawberry maturity recognition algorithm combining dark channel enhancement and yolov5," *Sensors*, vol. 22, no. 2, p. 419, 2022.
- [10] G. Liu, Z. Hou, H. Liu, J. Liu, W. Zhao, and K. Li, "Tomatodet: Anchor-free detector for tomato detection," *Frontiers in Plant Science*, vol. 13, p. 942875, 2022.
- [11] S. K. Behera, A. K. Rath, and P. K. Sethy, "Fruits yield estimation using faster r-cnn with miou," *Multimedia Tools and Applications*, vol. 80, no. 12, pp. 19043–19056, 2021.
- [12] J. Xiong, Z. Liu, R. Lin, R. Bu, Z. He, Z. Yang, and C. Liang, "Green grape detection and picking-point calculation in a night-time natural environment using a charge-coupled device (ccd) vision sensor with artificial illumination," *Sensors*, vol. 18, no. 4, p. 969, 2018.
- [13] J. Le Louëdec and G. Cielniak, "3d shape sensing and deep learning-based segmentation of strawberries," *Computers and Electronics in Agriculture*, vol. 190, p. 106374, 2021.
- [14] T. T. Santos, L. L. De Souza, A. A. dos Santos, and S. Avila, "Grape detection, segmentation, and tracking using deep neural networks and three-dimensional association," *Computers and Electronics in Agriculture*, vol. 170, p. 105247, 2020.
- [15] V. Tsironis, S. Bourou, and C. Stentoumis, "Tomatod: evaluation of object detection algorithms on a new real-world tomato dataset," *The International Archives of the Photogrammetry, Remote Sensing and Spatial Information Sciences*, vol. 43, pp. 1077–1084, 2020.
- [16] M. Afonso, H. Fonteijn, F. S. Fiorentin, D. Lensink, M. Mooij, N. Faber, G. Polder, and R. Wehrens, "Tomato fruit detection and counting in greenhouses using deep learning," *Frontiers in plant science*, vol. 11, p. 571299, 2020.
- [17] L. Cossio-Montefinale, J. Ruiz-del Solar, and R. Verschae, "Cherry co dataset: a dataset for cherry detection, segmentation and maturity recognition," *IEEE Robotics and Automation Letters*, 2024.
- [18] W. Jia, Z. Wang, Z. Zhang, X. Yang, S. Hou, and Y. Zheng, "A fast and efficient green apple object detection model based on foveabox," *Journal of King Saud University-Computer and Information Sciences*, vol. 34, no. 8, pp. 5156–5169, 2022.
- [19] L. Wu, J. Ma, Y. Zhao, and H. Liu, "Apple detection in complex scene using the improved yolov4 model," *Agronomy*, vol. 11, no. 3, p. 476, 2021.
- [20] H. Kang, H. Zhou, X. Wang, and C. Chen, "Real-time fruit recognition and grasping estimation for robotic apple harvesting," *Sensors*, vol. 20, no. 19, p. 5670, 2020.
- [21] S. Bhusal, M. Karkee, and Q. Zhang, "Apple dataset benchmark from orchard environment in modern fruiting wall," 2019.
- [22] N. Häni, P. Roy, and V. Isler, "Minneapolis: a benchmark dataset for apple detection and segmentation," *IEEE Robotics and Automation Letters*, vol. 5, no. 2, pp. 852–858, 2020.
- [23] M. Halstead, C. McCool, S. Denman, T. Perez, and C. Fookes, "Fruit quantity and ripeness estimation using a robotic vision system," *IEEE robotics and automation LETTERS*, vol. 3, no. 4, pp. 2995–3002, 2018.
- [24] C. Hou, X. Zhang, Y. Tang, J. Zhuang, Z. Tan, H. Huang, W. Chen, S. Wei, Y. He, and S. Luo, "Detection and localization of citrus fruit based on improved you only look once v5s and binocular vision in the orchard," *Frontiers in Plant Science*, vol. 13, p. 972445, 2022.
- [25] J. A. James, H. K. Manching, M. R. Mattia, K. D. Bowman, A. M. Hulse-Kemp, and W. J. Beksi, "Citdet: A benchmark dataset for citrus fruit detection," *arXiv preprint arXiv:2309.05645*, 2023.
- [26] S. Strautiņa, I. Kalniņa, E. Kaufmane, K. Sudars, I. Namatēvs, A. Nikulins, and E. Edelmers, "Raspberrysset: Dataset of annotated raspberry images for object detection," *Data*, vol. 8, no. 5, p. 86, 2023.
- [27] L. Zu, Y. Zhao, J. Liu, F. Su, Y. Zhang, and P. Liu, "Detection and segmentation of mature green tomatoes based on mask r-cnn with automatic image acquisition approach," *Sensors*, vol. 21, no. 23, p. 7842, 2021.
- [28] I. Sa, Z. Ge, F. Dayoub, B. Upcroft, T. Perez, and C. McCool, "Deepfruits: A fruit detection system using deep neural networks," *sensors*, vol. 16, no. 8, p. 1222, 2016.
- [29] J.-Y. Zhu, T. Park, P. Isola, and A. A. Efros, "Unpaired image-to-image translation using cycle-consistent adversarial networks," in *Proceedings of the IEEE international conference on computer vision*, 2017, pp. 2223–2232.
- [30] J. Grimm, K. Herzog, F. Rist, A. Kicherer, R. Toepfer, and V. Steinhage, "An adaptable approach to automated visual detection of plant organs with applications in grapevine breeding," *Biosystems Engineering*, vol. 183, pp. 170–183, 2019.
- [31] Y. Onishi, T. Yoshida, H. Kurita, T. Fukao, H. Arihara, and A. Iwai, "An automated fruit harvesting robot by using deep learning," *Robomech Journal*, vol. 6, no. 1, pp. 1–8, 2019.
- [32] B. Arad, J. Balendonck, R. Barth, O. Ben-Shahar, Y. Edan, T. Hellström, J. Hemming, P. Kurtser, O. Ringdahl, T. Tielens *et al.*, "Development of a sweet pepper harvesting robot," *Journal of Field Robotics*, vol. 37, no. 6, pp. 1027–1039, 2020.
- [33] C. Wilms, R. Johanson, and S. Frintrop, "Localizing small apples in complex apple orchard environments," *arXiv preprint arXiv:2202.11372*, 2022.
- [34] W. Zhang, J. Wang, Y. Liu, K. Chen, H. Li, Y. Duan, W. Wu, Y. Shi, and W. Guo, "Deep-learning-based in-field citrus fruit detection and tracking," *Horticulture Research*, vol. 9, p. uhac003, 2022.
- [35] J. F. Villacrés and F. Auat Cheein, "Detection and characterization of cherries: A deep learning usability case study in chile," *Agronomy*, vol. 10, no. 6, p. 835, 2020.
- [36] S. Bargoti and J. Underwood, "Deep fruit detection in orchards," in *2017 IEEE international conference on robotics and automation (ICRA)*. IEEE, 2017, pp. 3626–3633.
- [37] K. Schmidt, H. Höhn, B. Graf, and H. Höpli, "Phänologische entwicklungsstadien der himbeere (*rubus idaeus* l.)," *Forschung*, vol. 8, pp. 215–222, 2001.
- [38] Y. Zhang, X. Li, F. Wang, B. Wei, and L. Li, "A comprehensive review of one-stage networks for object detection," in *2021 IEEE International Conference on Signal Processing, Communications and Computing (ICSPCC)*. IEEE, 2021, pp. 1–6.
- [39] L. Du, R. Zhang, and X. Wang, "Overview of two-stage object detection algorithms," in *Journal of Physics: Conference Series*, vol. 1544, no. 1. IOP Publishing, 2020, p. 012033.
- [40] A. Wang, H. Chen, L. Liu, K. Chen, Z. Lin, J. Han, and G. Ding, "Yolov10: Real-time end-to-end object detection," *arXiv preprint arXiv:2405.14458*, 2024.
- [41] G. Jocher, A. Chaurasia, and J. Qiu, "Ultralytics YOLO," Jan. 2023. [Online]. Available: <https://github.com/ultralytics/ultralytics>
- [42] Y. Zhao, W. Lv, S. Xu, J. Wei, G. Wang, Q. Dang, Y. Liu, and J. Chen, "Detrs beat yolos on real-time object detection," in *Proceedings of the IEEE/CVF Conference on Computer Vision and Pattern Recognition*, 2024, pp. 16965–16974.
- [43] S. Ren, K. He, R. Girshick, and J. Sun, "Faster R-CNN: Towards real-time object detection with region proposal networks," *IEEE transactions on pattern analysis and machine intelligence*, vol. 39, no. 6, pp. 1137–1149, 2016.
- [44] K. He, G. Gkioxari, P. Dollár, and R. Girshick, "Mask R-CNN," in *Proceedings of the IEEE international conference on computer vision*, 2017, pp. 2961–2969.
- [45] N. Wouters, B. De Ketelaere, T. Deckers, J. De Baerdemaeker, and W. Saeys, "Multispectral detection of floral buds for automated thinning of pear," *Computers and Electronics in Agriculture*, vol. 113, pp. 93–103, 2015.
- [46] A. Botirov, S. An, O. Arakawa, and S. Zhang, "Application of a visible/near-infrared spectrometer indentifying flower and non-flower buds on 'fuji' apple trees," in *Library*, vol. 22, no. 2, pp. 214–219, 2022.
- [47] M. Asadi, K. Zareinia, and S. Saeedi, "Di-NeRF: Distributed nerf for collaborative learning with relative pose refinement," *IEEE Robotics and Automation Letters*, 2024.